Polish Journal of Chemical Technology, 19, 3, 1—8, 10.1515/pjct-2017-0040

Design, preparation and properties of novel flame retardant thermosetting vinyl ester copolymers based on castor oil and industrial dipentene

Wei Mao[1], Shouhai Li[1, 2*], Mei Li[1, 2], Kun Huang[1, 2], Jianling Xia[1, 2*]

[1]Institute of Chemical Industry of Forestry Products, CAF, Key Laboratory of Biomass Energy and Material, National Engineering Laboratory for Biomass Chemical Utilization, Key and Laboratory on Forest Chemical Engineering, SFA, Nanjing 210042, Jiangsu Province, China
[2]Institute of Forest New Technology, CAF, Beijing 10091,China
[*]Corresponding authors: e-mail: lishouhai1979@163.com; xiajianling@126.com

A novel bio-based flame-retardant thermosetting vinyl ester resin monomer was synthesized from castor oil. The chemical structures of the monomer was characterized by FTIR and 1H-NMR. In order to improve its rigidity and expand its application in the field of bio-based materials, it was mixed with certain proportions of another reactive bio-based VER monomer, which had rigid and strong polar groups, and then a series of copolymers were prepared with thermal curing method. Then their tensile property, hardness, morphology of fractured surface, flame retardant property, DMA and thermostability were all investigated. The results indicated that the copolymers had relatively high tensile strength of 11.2 MPa, and the limiting oxygen index is above 23% in all prepared copolymers. DMA demonstrates that the glass transition temperature of the cured resins is up to 56.1°C. Thermogravimetric analysis shows that the copolymers have excellent thermal stability.

Keywords: castor oil, vinyl ester resin, copolymers, flammability, thermal properties.

INTRODUCTION

Thermosetting vinyl ester resins (VERs) are a novel type of excellent resins that play a very important role in the industry due to their high curing degree, high cross-linking density, broad formulation and low energy consumption[1–5]. The cured materials of VERs are superior in mechanical properties, heat resistance, electrical properties and chemical stability than cheaper polyester resins[6–8]. In addition, the VERs are obtained from the reaction of an epoxy resin and an unsaturated carboxylic acid, which endow VERs with the excellent properties of both epoxy resins and unsaturated polyesters[9, 10]. Thus, VERs have gained growing attention.

Recently, because of fossil depletion and environmental pollution, renewable bio-based materials have attracted much attention, owing to high compatibility, low cost, annual renewability, low pollution, high added value and potential biodegradability[11–16]. Castor oil (CO) is a high-purity light-yellow oily liquid obtained from the seed of castor plant[17]. CO can form many useful derivatives through familiar organic reactions (Fig. 1)[18]. One major derivative is ricinoleic acid (RA), which has many functional groups, such as hydroxyl, carboxyl and unsaturated double bond groups[19–21].These functional groups can be epoxidized, esterified and hydrogenated, which makes RA a renewable chemical feedstock for preparation of fine chemical products, such as plasticizers, elastomer, biolubricant, polyurethane, and coating[17, 22]. As a byproduct from camphor preparation and pulp--paper industry, industrial dipentene is a very promising material with low price and high output[23]. This renewable material has many important and typical components, such as p-cymene, limonene, terpinolene, camphene, α-terpinene and other menthadienes (Fig. 2)[24]. With two reactive unsaturated double bond groups, industrial dipentene is a good candidate to prepare new products via Diels-Alder reaction, glycidylation, epoxy ring-opening reaction and esterification.

In addition, flammability becomes a major factor that hinders further development of VERs in some high--flame-retardancy applications[25–27]. The best method for improving flame retardance is to introduce reactive flame groups into the structures of VER monomers[28]. Among numerous flame retardants, P-containing flame retardants are the most commonly-used and are particularly effective for VERs[29]. In our previous work, retardant diglycidyl ester of maleinized dipentene modified with methacrylic anhydride and dibutyphosphate (MDDMD) (Fig. 3) VE monomer with rigid and strong polar groups was prepared[30]. Herein, we emphatically report a simple 'controllable esterification' strategy to prepare RA-based VE monomer for coatings. In order to improve the rigidity of RA-based coating, MDDMD was mixed into the RA-based monomer. Then we prepared series of thermosetting copolymers with different rigid-flexible characters from MDDRA(retardant diglycidyl ester of ricinoleic acid modified with methacrylic anhydride and dibutyphosphate) and MDDMD monomers. Their flammability, thermal properties and tensile properties were all investigated. This study can provide guidance for the design and manufacture techniques of this kind of coatings to some degree.

EXPERIMENTAL

Material

Ricinoleic acid (stabilized, 99.9%) was purchased from Nanjing Yixin Chemical Industry Co., Ltd., China and used as received. Epichlorohydrin (stabilized, 99.5%), methacrylic anhydride (stabilized, 99.5%), dibutyphosphate (stabilized, 99.5%), cobalt naphthenate (stabilized, 99.9) were purchased from Nanjing Kowloon Chemicals Co., Ltd., China and used as received. Benzyltriethylamine chloride (stabilized, 99.5%), sodium hydroxide (stabilized, 99%), triphenylphosphine (stabilized, 97%), calcium oxide (stabilized, 99.5), hydroquinone (stabilized,

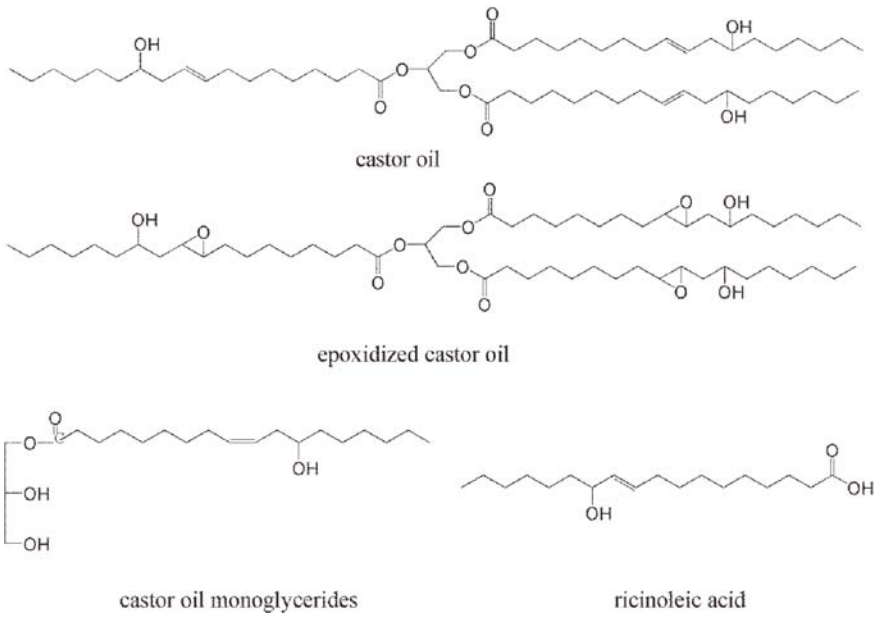

Figure 1. The molecular structure of castor oil and its derivatives

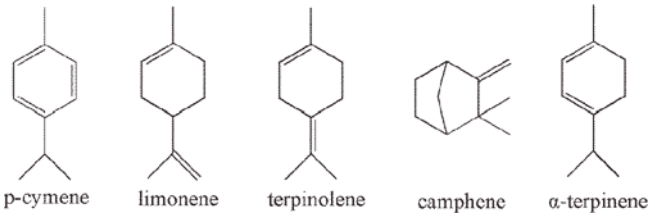

Figure 2. Chemical constituents of industrial dipentene

99%), poly(ethylene glycol) dimethacrylate-200 (PDA) (stabilized, 97%), benzoyl peroxide (stabilized, 73%) were purchased from Sinopharm Chemical Reagent Co., Ltd., China and used as received.

Synthesis of retardant diglycidyl ester of ricinoleic acid modified with methacrylic anhydride and dibutyphosphate (MDDRA)

First, 150.00 g of ricinoleic acid, 470.00 g of epichlorohydrin and 1.16 g of benzyltriethylamine chloride were added into a 1 L four-necked flask with a magnetic stirrer, a thermometer, a reflux condenser and a dropping funnel, and then heated to 115°C with mechanical stirring for 2 h. Then the mixture was cooled to 60°C, and 28.00 g of calcium oxide and 20.00 g sodium hydroxide were added to the flask with mechanical stirring and reacted for 3 h. Finally, the light yellowish diglycidyl ester of ricinoleic acid (DRA) was obtained by filtering and evaporating.

Then 20.00 g of DRA and 0.16 g of triphenylphosphine were weighed and put into a four-necked flask, and heated

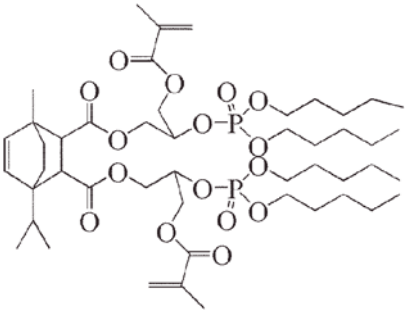

Figure 3. The molecular structure of MDDMD monomer

to 40–50°C with mechanical stirring, and then 11.86 g of dibutyphosphate was added slowly through a dropping funnel, and then heated to 70–75°C with mechanical stirring for 4 h, finally the yellow viscous ester (DDRA) was obtained. After that, 30.00 g of DDRA, 16.20 g of methacrylic anhydride, 0.24 g of hydroquinone and 0.48 g of triphenylphosphine were put into a four-necked flask, and was heated to 120°C and kept reacting for 2 h. Finally the dissociative methacrylic acid was removed by washing with distilled water and weak alkali, and then the residual water was removed by vacuum distillation, and then a yellow low-viscosity liquid resin (MDDRA) was obtained. The synthesis route is shown in Figure 4.

Preparation of thermal-cured copolymers

MDDRA, MDDMD and PDA (as a reactive diluent) were mixed uniformly by different weight ratios

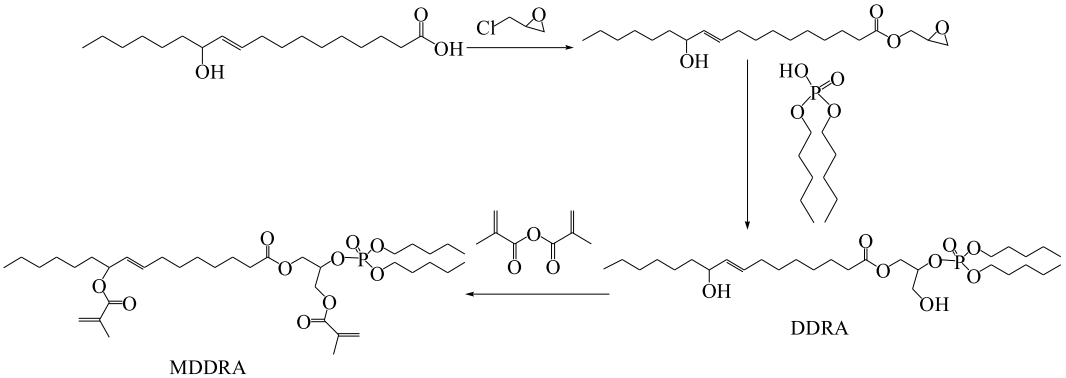

Figure 4. The synthesis route of MDDRA resin monomer

of 70%/0%/30%, 50%/20%/30%, 35%/35%/30%, 20%/50%/30% and 0%/70%/30% respectively. Then 2 wt% of benzoyl peroxide and 1 wt% of cobalt naphthenate were added as the radical initiator (2 wt% of the total resin weight). Cured samples were prepared by casting the above mixture into a vertical gasket molds. Then the molds cured into hot air oven at 120°C for 2 h and then post-cured 2 h at 140°C. The copolymers were denoted as follows: MDDRA70/MDDMD0/PDA30 means a mixture of 70 wt% MDDRA, 0 wt% MDDMD and 30 wt% PDA.

CHARACTERIZATION

FTIR analysis

The purified MDDRA was subjected to IS10 Fourier--transform infra-red (FTIR) spectroscopic analysis, to monitor the disappearance or formation of various functional groups in the wavelength range of 4000–400 cm^{-1}.

^{1}H nuclear magnetic resonance spectroscopy

^{1}H nuclear magnetic resonance (NMR) spectra of the purified MDDRA was recorded in $CDCl_3$ on an ARX300 spectrometer, operating at 500 MHz. Chemical shifts are given in ppm.

Tensile property testing of copolymers

Tensile properties of copolymers were measured by a CMT4303 universal test machine at a crosshead speed of 10 mm/min according to ASTM D638-03. And the test region of the samples was 50.0×13.0×3.2 mm^3. Five sample pieces were prepared for the sake of accuracy and all the samples were tested at 25°C.

Morphology of the fractured face

Scanning electron microscopy (SEM) observed on a 3400N Hitachi Co was used to investigate the tensile fractured face of copolymers. The specimens were mounted on an aluminum stub and sputter coated with a thin layer of gold to avoid electrostatic charging during examination.

Hardness of cured copolymers

The hardness of all the cured resins was measured by a TH 210 Shore D durometer at 25°C.

Flame retardant property

The limiting oxygen index (LOI) values were measured by a JF-3 oxygen index meter (Nanjing, China) according to ASTM D2863-97, and the test region of the samples was 130.0×6.5×3.2 m.

Dynamic mechanical thermal analysis (DMA)

The storage modulus and glass transition temperature were determined by a Q800 dynamic mechanical analyzer (DMA) in stretch test mode. All the cured resins had a dimension of 60.0×10.0×4.0 mm and were swept from –60 to120°C at a heating rate of 3°C/min as well as a frequency of 1 Hz.

Thermogravimetric analysis (TGA)

Thermal degradation characteristics and the percent weight loss of the cured resins were measured by a 409PC thermogravimetric analyzer (Netzsch, Germany). Each of samples was tested from 25 to 800°C at a rate of 15°C/min under a nitrogen atmosphere.

RESULT AND DISCUSSION

Fourier transform infrared (FTIR) analysis of MDDRA monomer

The FTIR spectra of DRA, DDRA and MDDRA are shown in Figure 5. As for DRA, the peaks at 2927 and 2855 cm^{-1} correspond to the antisymmetric and symmetric stretching vibrations, respectively, of C-H in -CH_3 and -CH_2-, and the peak at 1464 cm^{-1} corresponds to the bending vibration of C-H. In addition, the absorption peak of epoxy functional group at 856 cm^{-1} indicates the successful synthesis of DRA. On the spectra of DDRA, the strong peak at 3379 cm^{-1} corresponds to the hydroxyl stretching absorption, and its strong intensity indicates the formation of a hydroxy system among DDRA molecules. Other peaks appear at 1738 cm^{-1} (strong, corresponding to the stretching vibration of C=O from the ester groups), 1120 and 910 cm^{-1} (characteristic of P-O-C), 1030 cm^{-1} (P-O), and 1245 cm^{-1} (P=O). However, the peak of epoxy functional group at about 856 cm^{-1} and the characteristic peak of P-OH at 2600 cm^{-1} disappear. All these changes indicate the successful synthesis of DDRA. As for MDDRA, new absorption peaks of C=O at 1785 cm^{-1} and C=C at 1636 cm^{-1} appear, and the peak of O-H at 3410 cm^{-1} is weakened. All these changes indicate the successful reaction between DDRA and methacrylic anhydride to form MDDRA.

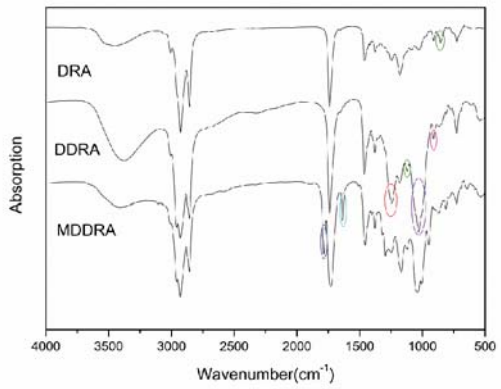

Figure 5. FTIR spectra of DRA, DDRA and MDDRA

^{1}H-nuclear magnetic resonance (^{1}H-NMR) analysis of MDDRA monomer

The ^{1}H-NMR spectra of DDRA and MDDRA are shown in Figure 6. For DDRA, the peaks at 3.9 and 4.41 ppm correspond to the protons on the epoxy group, indicating RA has reacted with epichlorohydrin. The strong peaks at about 2.0 ppm correspond to the protons of the hydroxyl group, which proves the occurrence of epoxy ring-opening. The peak at about 3.86 ppm corresponding to the methylene protons next to the hydroxyl group also indicates the occurrence of epoxy ring-opening. For MDDRA, the ^{1}H-NMR signal of the hydroxyl group at about 2.0 ppm disappears, which indicates the successful esterification between hydroxyl groups and methacrylic anhydride. The appearance of new peaks at 5.58 and 6.15 ppm corresponding to the protons of -CH=CH- further confirms the occurrence of esterification. In addition, the

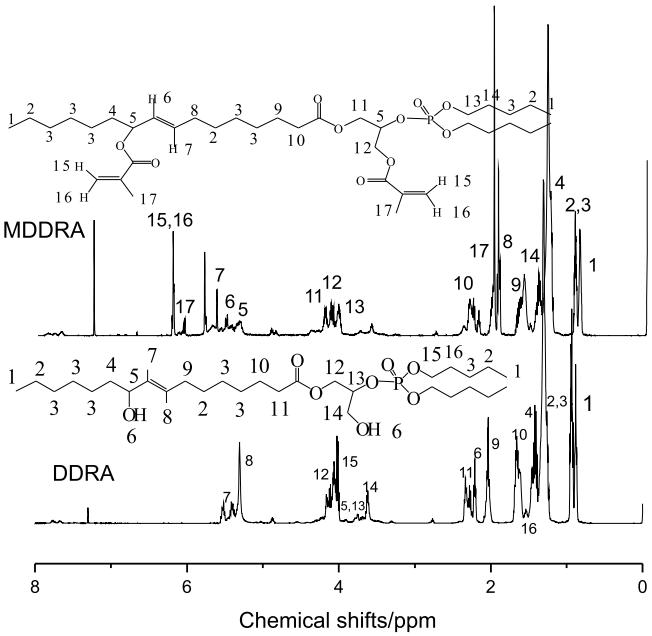

Figure 6. ^{1}H-NMR spectra of DDRA and MDDRA

shift of methyne protons from 3.90 to 4.64 ppm and the appearance of new peaks at 1.93 ppm of methyl protons also indicate the occurrence of esterification. All these ^{1}H-NMR results indicate that the target product has been successfully synthesized.

Tensile properties and hardness character of copolymers

Figure 7 shows the tensile stress-strain curves of the copolymers with different weight ratios. The details of tensile properties are summarized in Table 1. Clearly, the tensile stress-strain curves show that MDDRA70/PDA30 has the highest elongation at break and the lowest tensile strength, while MDDMD70/PDA30 shows the lowest elongation at break and the highest tensile strength, indicating MDDRA and MDDMD are characteristic of flexible and rigid materials, respectively. With the decrease of MDDRA content, the tensile strength increases, ranging from 1.9 to 11.2 MPa, while the elongation at break decreases, ranging from 35.5% to 13.1%. It is generally known that the tensile properties of the copolymers are simultaneously determined by the cross-linked state and the chemical structures of the copolymers. Compared with MDDRA, the rigid endocyclic structure of MDDMD monomer can endow the copolymerized system with higher tensile strength and lower elongation at break. With the increasing content of MDDRA monomer in copolymerized system, the content of flexible aliphatic chains structure increases, and the content of rigid endocyclic structure decreases, the rigidity of copolymerized system also decreases. In addition, the nonterminal double bond located on the endocyclic structure of MDDMD monomer also possess cross-linking curability. Thus the tensile stress-strain curves of the copolymers displayed such a changing trend.

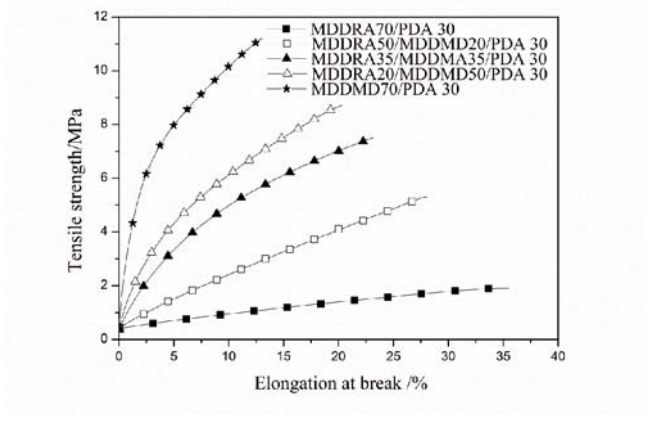

Figure 7. Tensile stress-strain curves of copolymers

Table 1 also shows the shore hardness of copolymers with different weight ratios. With the decrease of MDDRA content, the shore hardness of copolymers increases. This is mainly because the weight proportion of rigid alicylic hexatomic structure from MDDMD increases and proportion of long-chain flexible structure from MDDRA decreases with the increase of MDDMD content. This analysis result is consistent with the changing trend of tensile properties.

Morphology of the fractured surface

The morphologies of tensile fracture surfaces of copolymers were investigated by scanning electron microscopy (SEM). The SEM graphs displayed in Figure 8 show that the MDDMD70/PDA30 copolymerized system displays a brittle fractured character with smooth glass-like fractured surfaces, it is mainly because the MDDMD70/PDA30 cured system has more rigid alicyclic hexatomic structure. Moreover, the samples are uniformly forced with tensile rupture, so the copolymerized system has the characteristic of obvious fast fracture. On the contrary, with the increase of MDDRA monomer content, the surface flatness of copolymers decreases, and the shear zone of the crack branch is significantly enlarged. It could be explained by the fact that the cured MDDRA70/PDA30 system is a flexible material, so the increase of MDDRA content would reduce the surface flatness of copolymers.

Flame retardant property

The flammability of copolymers characterized by the limiting oxygen index (LOI) test is shown in Figure 9. LOI could determine the minimum oxygen concentration that supports the combustion of polymers. It is clear that LOIs are all above 23.1%, and the LOIs decrease from 27.2% to 23.1% with the increase of MDDRA content in copolymers. Compared with traditional VER

Table 1. Tensile properties and hardness of copolymers with different weight ratios

Samples	Tensile properties		Hardness
	strength [MPa]	elongation at break [%]	
MDDRA70/PDA 30	1.9±0.2	35.5±1.5	5.1
MDDRA50/MDDMD20/PDA 30	5.3±0.5	28.0±1.0	15.2
MDDRA35/MDDMD35/PDA 30	7.5±0.6	23.1±1.0	22.5
MDDRA20/MDDMD50/PDA 30	8.7±0.6	20.3±0.8	29.6
MDDMD70/PDA 30	11.2±0.6	13.1±0.6	40.2

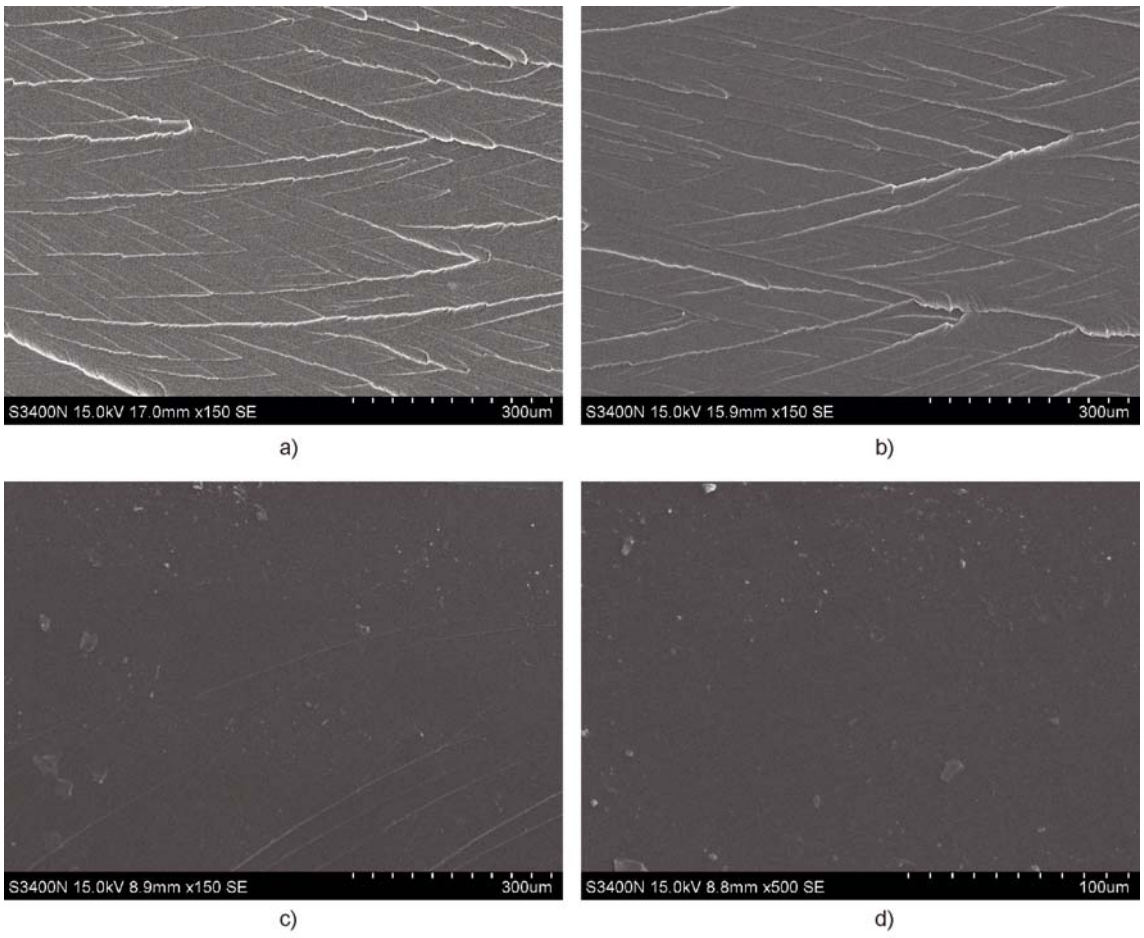

Figure 8. SEM micrographs of fracture surfaces of copolymers (a) MDDRA70/PDA30, (b) MDDRA35/MDDMD35/PDA30, (c, d) MDDMD 70/PDA30

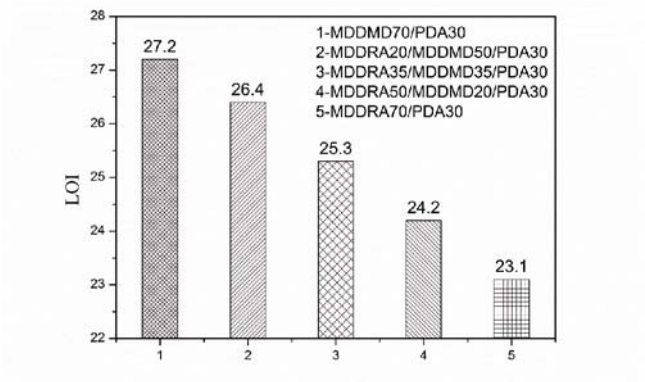

Figure 9. The LOI values of cured materials

copolymerized materials, the flammability of our prepared copolymers get improved to a certain extent. It concluded that the P content in MDDRA monomer is less than that in MDDMD monomer, and the P content rises from 3.12 wt% to 4.71 wt% with the decrease of MDDRA monomer content. As we know, P can both promote carbonization and inhibit combustion, a higher P content in the copolymers decelerates the burning and probably provides better flame protection for the copolymers. In addition, the rigid alicyclic hexatomic structure in copolymerized also could improve the flammability of copolymers. So the LOIs of copolymers increased with the decreasing content of MDDRA monomer in copolymerized system.

Dynamic mechanical thermal properties of copolymers

Figure 10 shows the storage modulus (E') and tanδ curves of copolymers with different weight ratios. Dynamic mechanical analysis (DMA) is a versatile thermal analysis technique to quantitatively study the viscoelastic behavior of cured copolymers. Clearly, the E' of the cured copolymers increases with the decrease of MDDRA content and the E' curves of all the cured copolymers show a similar trend. Briefly, at about –80°C, E' remains at a high level from 2250 to 3750 MPa, and with the temperature rise from –80 to 40°C, E' decreases and eventually all the E' values are close to a constant level below 100 MPa. The E' of prepared copolymers increased with the decreasing content of MDDRA monomer in copolymerized system. The cause could be consistent

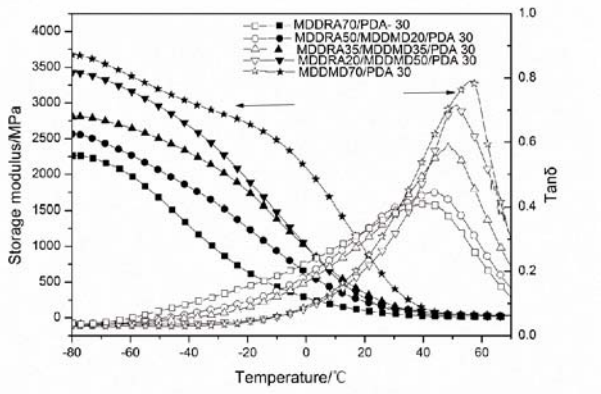

Figure 10. DMA curves of copolymers with different weight ratios

with the affecting factors of tensile properties. With the increase of MDDMD content, more flexible aliphatic chains from MDDRA are replaced by the rigid endocyclic structure from MDDMD, leading to a reduction of the free volume in the polymeric matrix and bestow the copolymers with certain high rigidity, and in this case chemical structure could be the main influence factor on the properties of the copolymerized system, so the MDDMD70/PDA30 system has higher E'.

E' is related to the crosslink density (ν_e) of cross-linked materials in the rubbery state, which could be used to calculate ν_e as follows:

$$\nu_e = E'/3RT$$

where E' is the storage modulus at T_g + 20°C, R is the gas constant and T is the absolute temperature at T_g + 20°C [31].

In order to ensure the copolymers are in the rubbery state, we set the temperature, where E′ was taken, at T_g + 20°C for each sample. Table 2 shows the crosslink density of the cured copolymers. Clearly, the ν_e of the cured copolymers increases with the increase of MDDMD content. Theoretically, the MDDRA monomer and the MDDMD monomer have two same reactive terminal double bonds, which are relatively structurally symmetrical in the MDDMD monomer and structurally unsymmetrical in the MDDRA monomer. And the relatively symmetrical structure in MDDMD monomer could make for improving the ν_e of the cured copolymers. In addition, the nonterminal double bond located on the endocyclic structure of MDDMD monomer also possess cross-linking reactivity. So the ν_e value of the cured copolymers increases with the increase of MDDMD content

Compared with MDDMD monomer, though MDDRA has a much small molecular structure, MDDRA monomer still has less reactive cross-linking point because MDDMD monomer has another reactive double-bonds located on alicylic hexatomic structure.

The peak temperature of tanδ corresponds to the glass transition temperature (T_g). On the tanδ curves (Fig. 10), each cured copolymer has a very clear single T_g, which indicate all the cured copolymers are compatible and have a homogeneously cross-linked structure (Fig. 11). Clearly, all the cured copolymers have a relatively high T_g up to 40.9–56.1°C, and T_g increases with the increase of MDDMD content, probably because of the molecular structures and cross-linked state of the copolymerized system, which is similar to the cause of mechanical proper-

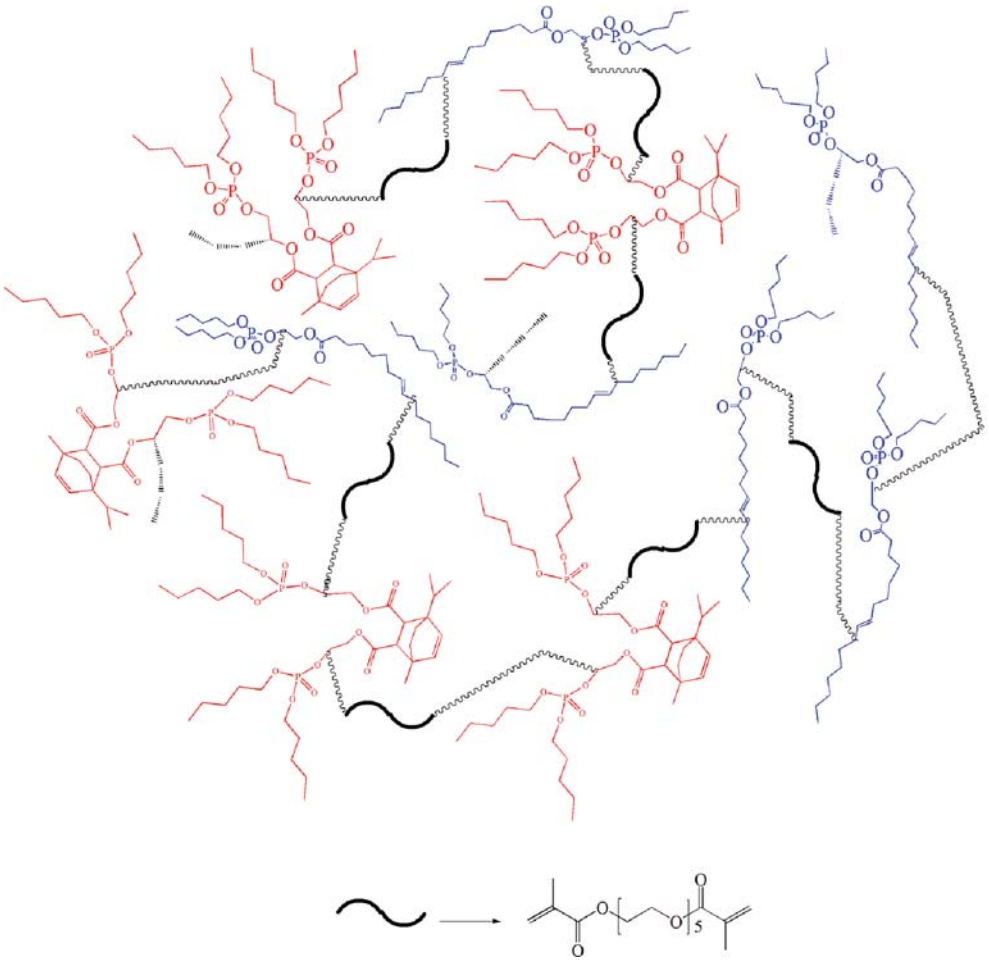

Figure 11. The possible crosslinking schematic diagram of copolymerized system

Table 2. The crosslink densities of copolymers with different weight ra

Samples	$T_{5\%}$ [°C]	T_i [°C]	T_{max} [°C]	T_f [°C]	Char yield [%]
MDDRA70/PDA 30	228	280.1	320.2	490	23.15
MDDRA50/MDDMD20/PDA 30	250	293.2	340.9	495	16.59
MDDRA35/MDDMD35/PDA 30	252	273.7	327.2	500	19.64
MDDRA20/MDDMD50/PDA 30	251	284.3	330.0	500	20.24
MDDMD70/PDA 30	266	307.0	346.9	500	13.12

ties. With the increasing content of MDDMD monomer, the introduction of more rigid and strong polar groups from alicyclic groups somehow overcome the action of long fatty acid chains on copolymerized system, so the T_g increases with the increase of MDDMD content. In addition, with higher MDDRA content, the molecular chains of the cured system become more mobile, and relaxing process of molecular chains is prolonged, so the tanδ curves show wider and lower peaks.

The thermal stability of the cross-linked networks plays a very important role and is greatly influenced by the molecular structure, concentration and type of the remaining polar groups, chemical composition, and molecular chain rigidity. Figure 12 shows the TGA curves of copolymers with different weight ratios. The initial decomposition temperature (T_i), temperature of maximum mass loss (T_{max}), final decomposition temperature (T_f) and the char yield at 800°C are all listed in Table 3. Clearly, all the copolymers are thermally stable even up to 200°C and all the TGA curves display a single-step mass loss decomposition behavior.

Weight loss started at above 273°C in all the cured copolymers, while the final char yields of the copolymers are all above 13.1%, indicating that all the copolymers have high thermostability. The mass loss might be attributed to the thermal degradation of dibutyphosphate groups on MDDRA and MDDMD, as well as the rupture of ester groups and C-C groups from MDDRA and MDDMD. The thermograms (Table 3) show that the concentrations of MDDMD do not much affect the nature of cross-links formed during curing, so the T_i and T_{max} are both close between the two mixed resins with different MDDRA/MDDMD weight ratios. The thermostability of MDDMD70/PDA30 is higher compared with other mixed copolymerized systems. The high thermostability of MDDMD70/PDA30 is probably attributed to the large proportions of rigid alicyclic structures and endocyclic structures, which delay the decomposition of copolymer and subsequent diffusion of decomposition products. Moreover, all the data do not display a good uptrend, but the reasons are complex. For different curing copolymers, the molecular structure of mixed monomers, curing degree and crosslink density can affect the thermostability of copolymers. Thus, the thermostability of prepared copolymers changes irregularly.

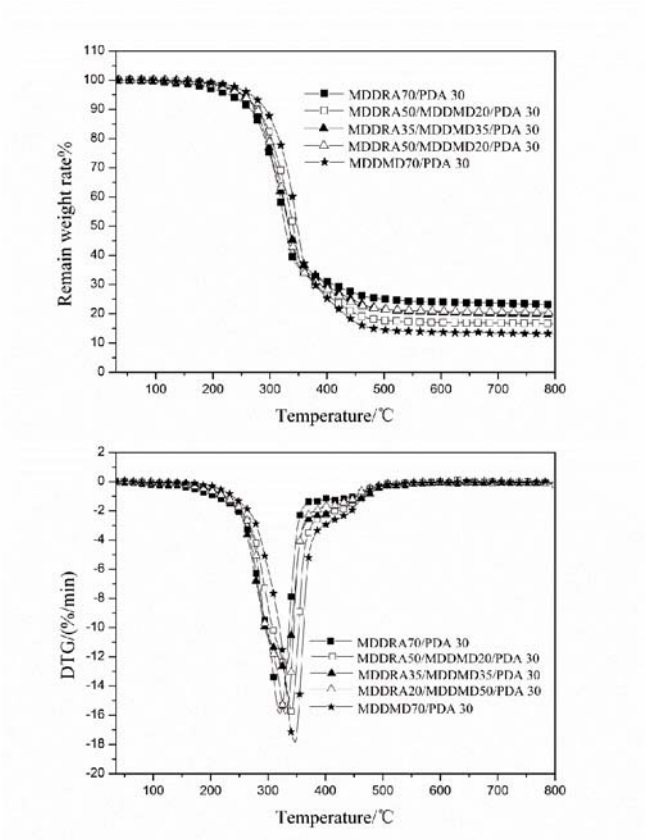

Figure 12. TG analysis curves of copolymers with different weight ratios

Table 3. TG analysis data of copolymers with different weight ratios

Samples	$T_{5\%}$ [°C]	T_i [°C]	T_{max} [°C]	T_f [°C]	Char yield [%]
MDDRA70/PDA 30	228	280.1	320.2	490	23.15
MDDRA50/MDDMD20/PDA 30	250	293.2	340.9	495	16.59
MDDRA35/MDDMD35/PDA 30	252	273.7	327.2	500	19.64
MDDRA20/MDDMD50/PDA 30	251	284.3	330.0	500	20.24
MDDMD70/PDA 30	266	307.0	346.9	500	13.12

CONCLUSIONS

A novel bio-based VER monomers named MDDRA and a series of copolymers containing MDDRA, MDDMD and PDA were successfully prepared. It was proved that MDDRA70/PDA30 was a flexible material with relatively low tensile strength, modulus and hardness, while MDDMD70/PDA30 was a rigid material with relatively high tensile strength, modulus and thermal stability. The hardness of cured resins ranged from 40.2 to 5.1 HD and the LOIs varied from 27.2 to 23.1 with the increase of MDDRA content. DMA shows that the glass-transition temperatures of the copolymers increased from 40.9 to 56.1°C with the increase of MDDMD content. TGA demonstrated that the copolymers containing higher content of MDDMD had higher thermal stability, and the thermal initial degradable temperatures of the copolymers were all above 270°C, demonstrating the high thermal stability of all the copolymers. All the evidence demonstrated that the addition of MDDRA monomer could improve the toughness of copolymerized system. This study presents a perfect combination of rigid alicyclic structure and flexible aliphatic chain structure. It also has significant implications for the design of fully bio-based novel flame retardant thermosetting vinyl ester copolymers with desired properties.

ACKNOWLEDGEMENTS

This work was supported by National Nonprofit Institute Research Grant of CAFINT (Grant Number: CAFINT2014C08).

LITERATURE CITED

1. Raquez, J.M., Deleglise, M., Lacrampe, M.F. & Krawczak, P. (2010). Thermosetting (bio) materials derived from renewable resources: a critical review. *Prog. Polym. Sci*. 35, 487–509. DOI: 10.1016/j.progpolymsci.2010.01.001.

2. Yousefi, A., Lafleur, P.G. & Gauvinm R. (1997). Kinetic studies of thermoset cure reactions: a review. *Polym. Comp.*18, 157–168. DOI: 10.1002/pc.10270.

3. Sultania, M., Yadaw, S.B., Rai, J.S.P. & Srivastava, D. (2010). Laminates based on vinyl ester resin and glass fabric: A study on the thermal, mechanical and morphological characteristics. *Mater. Sci. Eng. A*. 527, 4560–4570. DOI: 10.1016/j.msea.2010.04.038.

4. Boyard, N., Vayer, M., Sinturel,C., Erre, R. & Levitz, P. (2005). Study of the porous network developed during curing of thermoset blends containing low molar weight saturated polyester. *Polymer*. 46, 661–669. DOI: 10.1016/j.polymer.2004.11.094.

5. Li, S., Yang, X., Huang, K., Li, M. & Xia, J. (2014). Design, preparation and properties of novel renewable UV-curable copolymers based on cardanol and dimer fatty acids. *Prog. Org. Coat*. 77, 388–394. DOI: 10.1016/j.porgcoat.2013.11.011.

6. Yang, X., Li, S., Xia, J., Song, J., Huang, K. & Li, M. (2015). Novel renewable resource-based UV-curable copolymers derived from myrcene and tung oil: preparation, characterization and properties. *Ind. Crop. Prod*. 63, 17–25. DOI: 10.1016/j.indcrop.2014.10.024.

7. Benmokrane, B., Ali, A.H., Mohamed, H.M., EISafty, A. & Manalo, A. (2017). Laboratory assessment and durability performance of vinyl-ester, polyester, and epoxy glass-FRP bars for concrete structures. *Compos. Part. B. Eng.* DOI: 10.1016/j.compositesb.2017.02.002.

8. Afshar, A. Liao, H.T., Chiang, F.P. & Korach, C.S. (2016). Time-dependent changes in mechanical properties of carbon fiber vinyl ester composites exposed to marine environments. *Compos. Struct*. 144, 80–85. DOI: 10.1016/j.compstruct.2016.02.053.

9. Can, E., Kinaci, E. & Palmese, G.R. (2015). Preparation and characterization of novel vinyl ester formulations derived from cardanol. *Eur. Polym. J*. 72, 129–147. DOI: 10.1016/j.eurpolymj.2015.09.010.

10. Sultania, M., Rai, J.S.P. & Srivastava, D. (2009). Synthesis and curing of cardanol-based vinyl ester resins for applications in surface coatings-I. *Paint. India*. 9, 89–108.

11. Ummartyotin, S. & Pechyen, C. (2016). Strategies for development and implementation of bio-based materials as effective renewable resources of energy: A comprehensive review on adsorbent technology. *Renew. Sust. Energ. Rev.* 62, 654–664. DOI: 10.1016/j.rser.2016.04.066.

12. Kummerer, K. (2007). Sustainable from the very beginning: rational design of molecules by life cycle engineering as an important approach for green pharmacy and green chemistry. *Green. Chem.* 9, 899–907. DOI: 10.1039/B618298B.

13. Chiari, L. & Zecca, A. (2011). Constraints of fossil fules depletion on global warming projections. *Energy. Policy*. 39, 5026–5034. DOI: 10.1016/j.enpol.2011.06.011.

14. Do, H., Park, J.H. & Kim, H.J. (2008). UV-curing behavior and adhesion performance of polumeric photoinitiators blended with hydrogenated rosin epoxy methacrylate for UV--crosslinkable acrylic pressure sensitive adhesives. *Eur. Polym. J*. 44, 3871–3882. DOI: 10.1016/j.eurpolymj.2008.07.046.

15. Gobin, M., Loulergue, P., Audic, J.L. & Lemiegre, L. (2015). Synthesis and characterization of bio-based polyester materials from vegetable oil and short to long chain dicarboxylic acids**.** *Ind. Crop. Prod*. 70, 213–220. DOI: 10.1016/j.indcrop.2015.03.041.

16. Konwar, U., Karak, N. & Mandal, M. (2010). Vegetable oil based highly branched polyester/clay silver nanocomposites as antimicrobial surface coating materials. *Prog. Org. Coat*. 68, 265–273. DOI: 10.1016/j.porgcoat.2010.04.001.

17. Ebata, H., Yasuda, M., Toshima, K. & Matsumura, S. (2008). Poly (ricinoleic acid) based novel thermosetting elastomer. *J. Oleo. Sci*. 57, 315–320. DOI: 10.5650/jos.57.315.

18. Park, S.J. Jin, F.L. & Lee, J.R. (2004). Effect of biodegradable epoxidized castor oil on physicochemical and mechanical properties of epoxy resins. *Macromol. Chem. Phys*. 205, 2048–2054. DOI: 10.1002/macp.200400214.

19. Behr, A., Krema, S. & Kamper, A. (2012). Ethenolysis of ricinoleic acid methyl ester-an efficient way to the olechemical key substance methyl dec-9-enoate. *RSC. Adv*. 2, 12775–12781. DOI: 10.1039/C2RA22499B.

20. Chandorkar, Y., Mards, G. & Basu, B. (2013). Structure, tensile properties and cytotoxicity assessment of sebacic acid based biodegradable polyesters with ricinoleic acid. *J. Mater. Chem. B*. 1, 865–875. DOI: 10.1039/C2TB00304J.

21. Krasko, M.Y., Shikanow, A., Ezra, A. & Domb, A.J. (2003). Poly (ester anhydride) s prepared by the insertion of ricinoleic acid into poly(sebacic acid). *J. Polym. Sci. Part. A: Polym. Chem*. 41, 1059–1069. DOI: 10.1002/pola.10651.

22. Salimon, J. & Salih, N. (2010). Modification of epoxidized ricinoleic acid for biolubricant base oil with improved flash and pour points. *Asian. J. Chem*. 22, 5468–5476.

23. Lesage, P., Candy, J.P. & Hirigoyen, C. (1996). Selectve dehydrogenation of dipentene(R-(+)-limonene) into paracymene on silica supported palladium assisted by α-olefins as hydrogen acceptor. *J. Mol. Cata. A: Chem*. 112, 431–435. DOI: 10.1016/1381-1169(96)00220-8.

24. Zhang, Q., Bi, L., Zhao, Z., Chen, Y., Li, D., Gu, Y., Wang, J., Chen, Y., Bo, C. & Liu, X. (2010). Application of ultrasonic spraying in preparation of p-cymene by industrial dipentene dehydrogention. *Chem. Eng. J*. 159, 190–194. DOI: 10.1016/j.cej.2010.02.052.

25. Zhang, L., Zhang, M., Hu, L. & Zhou, Y. (2014). Synthesis of rigid polyurethane foams with castor oil-based flame retardant polyols. *Ind. Crop. Prod*. 52, 380–388. DOI: 10.1016/j.indcrop.2013.10.043.

26 Qian, L., Ye, L., Xu, G., Liu, J. & Guo, J. (2011). The non-halogen flame retardant epoxy resin based on a novel compound with phosphaphenanthrene and cyclotriphosphazene double functional groups. *Polym. Degrad. Stab*. 96, 1118–1124. DOI: 10.1016/j.polymdegradstab.2011.03.001.

27. Zhang, L., Zhang, M., Zhou, Y. & Hu, L. (2013). The study of mechanical behavior and flame retardancy of castor oil phosphate-based rigid polyurethane foam composites containing expanded graphite and triethyl phosphate. *Polym. Degrad. Stab*. 98, 2784–2794. DOI: 10.1016/j.polymdegradstab.2013.10.015.

28. Gao, L., Wang, D., Wang, Y., Wang, J. & Yang, B. (2008). A flame-retardant epoxy resin based on a reactive phosphorus-containing monomer of DODPP and its thermal and flame-retardant properties. *Polym. Degrad. Stab*. 93, 1308–1315. DOI: 10.1016/j.polymdegradstab.2008.04.004.

29. Laoutid, F., Bonnaud, L., Alexandre, M., Lopez-Cuesta & Dubois, J.M. (2009). New prospects in flame retardant polymer materials: from fundamentals to nanocomposites. *Mater. Sci. Eng. A*. 63, 100–125. DOI: 10.1016/j.mser.2008.09.002.

30. Mao, W., Li, S., Li, M., Yang, X., Song, J., Wang, M., Xia, J. & Huang, K. (2016). A Novel Flame Retardant UV-Curable Vinyl Ester Resin Monomer based on Industrial Dipentene: Preparation, Characterization and Properties. *J. Appl. Polym. Sci.* 133. DOI: 10.1002/app.44084.

31. Asif, A., Shi, W., Shen, X. & Nie, K. (2005). Physical and thermal properties of UV curable waterborne polyurethane dispersions incorporating hyperbranched alipatic polyester of varying generation number. *Polymer* 46, 11066–11078. DOI: 10.1016/j.polymer.2005.09.046.